*Article*

# Authentication of a Bronze Bust of Napoleon I, Attributed to Renzo Colombo from 1885

Ion Sandu [1,2,3,4], Vasile Drobota [5,6,*], Ana Drob [3], Andrei Victor Sandu [1,2,4,7,*], Viorica Vasilache [3], Cosmin Tudor Iurcovschi [4] and Ioan Gabriel Sandu [7,*]

1   Academy of Romanian Scientists (AORS), 54 Splaiul Independenței St., Sector 5, 050094 Bucharest, Romania; ion.sandu@uaic.ro
2   National Institute for Research and Development in Environmental Protection, 294 Splaiul Independenței, 6th District, 060031 Bucharest, Romania
3   Science Department, Interdisciplinary Research Institute, Alexandru Ioan Cuza University, 11 Carol I Blvd, 700506 Iași, Romania; anadrob1@gmail.com (A.D.); viorica_18v@yahoo.com (V.V.)
4   Romanian Inventors Forum, 3 Sf. Petru Movilă St., L11, III/3, 700089 Iași, Romania; tudor460@yahoo.com
5   Geoscience PhD School, Geography-Geology Faculty, Alexandru Ioan Cuza University, 11 Carol I Bulevard, 700506 Iași, Romania
6   Iasi County Police Inspectorate, Str. Mihai Costăchescu, nr. 2, 700495 Iași, Romania
7   Faculty of Materials Science and Engineering, Gheorghe Asachi Technical University of Iasi, 67 Dimitrie Mangeron Blvd, 700050 Iasi, Romania
*   Correspondence: drobotavasile@yahoo.com (V.D.); andrei-victor.sandu@academic.tuiasi.ro (A.V.S.); ioan-gabriel.sandu@academic.tuiasi.ro (I.G.S.)

**Abstract:** This paper presents the authentication analysis of a bronze bust of Napoleon I, attributed to the Italian artist Renzo Colombo (1856–1885) based on his signature and other casting and molding inscriptions. The bust was made using the lost wax technique and artificially patinated in the Pinédo variant workshop. This study combined historiographical research (using the specialized literature) with data from auction catalogs. These were compared with photographs of the entire bust and close-up images of key areas, including anthropomorphic features, clothing, inscriptions, and structural and ornamental details. The condition of the bust and its historical and chemical characteristics were assessed through direct analysis with magnifying tools and indirect analysis using scanning electron microscopy with energy-dispersive X-ray spectroscopy (SEM-EDX).

## 1. Introduction

Today, the illegal counterfeiting of works of art or archaeological artifacts is the third most important illegal activity in terms of revenue, after drugs and arms trade [1–3].

The counterfeiting and forgery of works of art are motivated by personal, sentimental, religious, truthful, onerous, practical, and scientific motives. In general, the purpose of these types of illegal activity can also take different forms, from the sentimental–personal to the pecuniary. As previously mentioned, when the reproduction of an authentic work is intended for trafficking and selling it as an original for profit, it constitutes a forgery rather than a scientific copy, which serves different purposes [4,5].

Today, we are also witnessing an atypical phenomenon, with many large collections, public or private, owning fake works of art or archaeological pieces but not declaring them for various reasons, of which an important place is held by the economic one, which is inextricably linked to the works' image and value [1].

In general, forgeries embody the defining features of a particular style, reproducing the faithful characteristics of an "authentic original", and are easily convincing to buyers, art dealers, or collectors. It often refers not only to the artwork itself, including aspects like

the signature and date, but also to other elements or modifications, such as repainting or refinishing, structural and color reintegration, as well as additional alterations or insertions made over time [1,3].

It is recognized that certain products of human activity, reflecting talent, creativity, and craftsmanship, have been transformed into cultural heritage objects and genuine historical testimonies. Beyond their inherent heritage qualities—such as age, value, author or workshop, artistic technique, technology, and historical patina—these objects have acquired, over time, significant heritage functions. These functions make them invaluable and irreplaceable from aesthetic–artistic, historical–documentary, technical–scientific, socioeconomic, and architectural perspectives, even embodying the highest form of identity for a community or individual: the spiritual dimension [3–5].

As mentioned above, the authentication of a work of art is not only about dating and establishing the author/studio/school but much more: determining the route from commissioning to collection/museum, with all its historical contexts and structural–functional evolution/physical, aesthetic, and conceptual state, along with a series of attributes related to the area of commissioning and use, ownership (owner/custodian/gallery/museum), itineraries, heritage value, etc. [6,7].

In the complex task of authenticating works of art today, the art historian or art critic, the so-called traditional expert, is powerless without the collaboration of technical–scientific experts from related fields (chemistry, physics, biology, geology, archaeology, anthropology, etc.).

Through the investigation of certain archaeometric characteristics or the identification with attribution of chemometric ones with archaeometric value, dating is realized, and through aesthetic–artistic analysis, it is possible to establish the author, school, workshop, etc. Using instrumental methods, the nature of the materials is determined, and their state of conservation or that of their structural components is established. By intrinsic and exhaustive analysis of the evolutionary effects of deterioration, which affect the physical state of the structural–functional elements, and those of degradation, which change the chemical nature of the component materials, it is possible to establish the two groups of attributes: the heritage elements or characteristics and the heritage functions, which are very important in determining authenticity [8–12].

No references to Renzo Colombo's bronzes were found in the specialized literature within scientific journals. However, numerous monographs exist that discuss the artist's life and work, including studies specifically on the bust of Napoleon I [13–19].

The literature on the study of ancient bronze alloys, statue casting processes, and patination is vast. The most representative works on these topics are presented below.

The first step in establishing the authenticity of a Renaissance bronze statue is a comprehensive study of the alloy composition, patina, dirt deposits, deterioration, and degradation due to exogenous factors and agents, including anthropogenic factors, through handling or interventions after the commissioning [20].

Establishing the composition of the base alloy and the patina, together with visual observations of the statue's interior and exterior, allows for revealing the way it was cast (lost wax casting technique) and the artificial patination process, respectively, as well as the origin of the raw materials (mineral processing, alloy elaboration), the contexts of casting and use, and the evolution of the state of conservation [21].

Concerning the originals and replicas/copies, a detailed scientific study confirms several issues related to the iconography and identity of the figure/character and whether they were made in the same workshop or different in terms of area or time. Moreover, the study provides further evidence of the heterogeneity and ingenuity of artistic bronze production for the Renaissance period and whether the artist themselves was involved in the technical aspects of the work [22–28].

Concerning the evolution of the state of conservation based on a multidisciplinary analysis, correlation hypotheses relevant to the patina and the deterioration and degradation processes that have occurred are possible [29].

Involvement of an interdisciplinary analytical protocol, with non-invasive analysis, provides essential information to correctly assign archaeometric and chemometric characteristics, changes in alloy phases and patina (surface contamination), missing structural elements through loss and neglect, etc. [30–41].

Knowing that a common procedure to protect bronze surfaces after casting is to coat them with an artificial patina, with corrosion protection and aesthetic value, involving precipitation by cementation with chemical reagents or electrochemical processes when thin, uniform, and continuous films of highly stable and insoluble stoneware-type oxides, hydroxides, chlorides, sulfides, sulfites, sulfates, nitrates, and phosphates result [42–46]. The elemental composition analysis provides sufficient data for the alloy type and artificial patina determination. The first evidence of the use of artificial patina dates to antiquity. Such patinas are dated from the Bronze Age and were discovered in China, indicating that chemicals are deliberately applied on the artifact's surface [45,46].

The main reagents used over time for bronze patinating are copper and manganese sulfate, potassium permanganate, hydroalcoholic ammonia solution, sodium thiosulfate, zinc chloride, ammonium sulfide, potassium sulfide, sodium hydrogen carbonate or sodium dicarbonate, hydrochloric acid, sulfuric acid, nitric acid, nitric acid, phosphoric acid, potassium or sodium dichromate, ferric chloride, stibium pentasulfide, sulfuric ointment, Renaissance wax or wax in the form of blue paste, etc. Based on recipes, little-known artificial brown patinas, known as Florentine, were made and widely used during the Renaissance period, when they became very popular in 15th–18th century Italy [47–50].

The final quality of a natural patina varies depending on the alloy's composition, the artifact's age, and the environmental conditions in which the artifact has been preserved. Chemically, the multilayer film can be described in its primary form as a hydrated copper oxide, stabilized on a copper suboxide substrate or composed mainly of a series of ultrathin, layered, statistically distributed stable or metastable ultrathin phases corresponding to the minerals listed below, as a congruent or summative system (one or more structurally integrated minerals). The literature abounds in a very large number of reference compounds, $CuO$ (*Tenorite*), $Cu_2O$ (*Cuprite* or *Ruberite*), $Cu_2S$ (*Chalcocite* or *Chalcozine*), $CuS$ (*Covellite*), $Cu_2 FeSnS_4$ (*Stanitte*), $SnO$ (*Romarchite*), $SnO_2$ (*Casitterite*), $Cu_2 Cl_2$ (*Nantochite*), $Cu_2 (OH)_3 Cl$ (with two allotropic forms: *Athacamit and Clinoathacamit*), $Cu_2(OH)_3NO_3$ (*Gerhardtite*), $CuSO_4 \cdot 3Cu(OH)_2 / Cu_4(OH)_6SO_4$ (*Brochantit*) $CuCl_2 \cdot 2H_2O$ (*Eriochalcite*), $Cu_2(OH)_2CO_3$ (*Malachite*), $Cu_3(OH)_2(CO_3)_2$ (*Azurite*), $CuSO_4 \cdot 5H_2O$ (with two allotropic forms: *Anthlerite and Chalcanthite*), $Cu_4(OH)_6SO_4 \cdot 2H_2O$ (*Langit*), and $Cu_{19}(OH)_{32}(SO_4)Cl_4 \cdot 3H_2O$ (*Connelite*), of which the most common are the sulfate- and copper chloride-based patinas, together with oxides, chlorides and sulfides, with segregated traces of tin oxides (*Romarchite* and *Cassiterite*) [51–55].

Being a synthetic or artificial patina, it often consists of only a few mineral phases composed mostly of Chalcanthite, Cuprit (Ruberite) + Chalcanthite, or Antlerite + Brochantite + Chalcanthite [56–60].

The specific artificial patina for quaternary bronze (Cu-Zn-Sn-Pb), allows for a special aesthetic, characterized by superior chromaticity and reflectance and stopping the formation of copper trihydroxychloride—$Cu_2(OH)_3Cl$—known as *bronze disease* (unstable over time), but which, with appropriate treatment, creates protective species of *Atacamite*: *Paratacamite* and *Clinoatacamite* [61,62]. *Nantokite* protects the inside of the pitting by preventing oxygen diffusion through forming the protective *Cuprite* patina [63].

The artificial brown patina of the Renaissance type, which has mainly an aesthetic but also a protective role, was long thought to have an unknown composition. Its structure had numerous constituent phases arranged in a single or several thin layers, depending on the application process.

Multi-instrumental analysis data, with reference to the natural noble patina, taken as a reference in the realization of the artificial one, revealed that the most common one is formed by copper oxides (Cuprit and Tenorite), basic copper nitrate (Gerhardtite), basic

copper sulfate (Brochantite), hydroxo sulfate trihydrate, and copper chloride (Connelit), which result in time under acid rain conditions [64–66].

The patination or coloring of cast bronze adds a certain aesthetic value to the artifact and provides anti-corrosive protection. The history of art shows that over the centuries, various ways of achieving an artificial patina immediately after casting and finishing have been preferred, ranging from white, blue–green, and brown to red and black.

Since the specialized literature presents many compositional formulations assisted by various operations, they will be briefly detailed in tabular form (Table 1) to facilitate their presentation.

**Table 1.** Correlation between artificial patina color for bronze artifacts and the nature of surface treatment solutions and operations.

| Patina Hue | Composition of Solutions and Treatment Operations |
| --- | --- |
| Dark brown * | An aqueous mixture of potassium sulfide, barium sulfide, and liquid ammonia or 1 part antimony sulfide, 1 part sodium hydroxide (lye), and 32 parts water, brought to a temperature of 93 °C. applied to the hot piece or 1 part copper sulfate, 1 part potassium chlorate, and 16 parts water, all mixed at room temperature and applied to the cold piece. |
| Reddish brown * | Aqueous solution of yellow barium sulfide and water, heated to 65.5 °C or 5 parts copper sulfate, 2 parts acetic acid, 2 parts sodium hydroxide (lye), and 65 parts water, at 71.1 °C |
| Black * | Arsenic acid 2 parts, 4 parts muriatic acid, 1 part sulfuric acid and 64 parts water or 2 parts copper carbonate, 4 parts ammonium hydroxide, 1 part sodium carbonate, and 32 parts water; the solution is heated to 66–67 °C |
| Bluish green * | Mixture of sodium sulfate and iron nitrate dissolved in water (ratio 4:1:5) or 4 parts sodium sulfate, 1 part sodium sulfate, 1 part iron nitrate, and 64 parts water, the solution is heated to 80 °C and the piece is kept immersed until the desired color appears; or 1 part copper nitrate, 1 part ammonium chloride, 1 part calcium chloride, and 32 parts water, the mixture is used at room temperature; or 8 parts copper sulfate, 4 parts ammonium chloride, 4 parts sodium chloride, 1 part zinc chloride, 3 parts acetic acid, and 128 parts water at normal temperature (for a more rapid effect by gentle heating). |
| Ancient green * | Hot aqueous solution of copper sulfate, ammonium chloride (12:1) or 14 parts ammonium chloride, 3 parts iron chloride, 8 parts sodium chloride, 8 parts green pigment, 4 parts potassium bitartrate, and 128 parts water; the solution should be heated to 93 °C and applied to the heated piece (the higher the concentration, the more intense the color) |
| Raw greens * | Aqueous mixture of sodium chloride, liquid ammonia, ammonium chloride, and vinegar. |
| Yellow greens * | Mixture of ammonium chloride, copper acetate, and water. |
| Blue * | 4 parts sodium sulfate, 3 parts lead acetate and 64 parts water, all heated to 82 °C, or use a mixture of 1 part ammonium chloride and 1 part copper nitrate dissolved in 32 parts water |

* For alterations to the basic hue, ammonium hydroxide is added in certain parts to the above solutions.

The most popular recipe today for the reddish-brown color is made from roasted caustic soda with the flower of sulfur in fine granules, which are dispersed in water and diluted to the desired solution (keep in the dark until use).

It is also known that artifacts with fine surfaces obtained by the lost wax technique are artificially patinated immediately after casting and chiseling, either by applying the treatment at room temperature or at higher temperatures when the artifact is heated in the kiln or by flaming. After maturation of the patina, the warm artifact is immersed in wax; paraffin; or optimal compositions of wax, paraffin, and molten rosin; or a dilute organic solution of wax in turpentine is applied at normal temperature. In all cases, after these processes, the artifact is wiped with soft/flaked (non-woven) textiles [8–12]. These protective films give the piece a special shine and protect it from contact with substances that attack the surface. A protective layer of natural or synthetic varnish may often be applied, but only to indoor artifacts.

Like any artifact of cultural heritage, each object is unique and has, after being put to work, a well-differentiated behavior over time, given by the elemental or phasal composition, casting technique, temperature, processes of artificial patination or natural patination, and the surface deposits of dirt accumulated over time. Based on the knowledge of the formation and evolution of natural bronze patinas, since the Middle Ages, artificial patinas have been synthesized for bronze and brass pieces, culminating in the modern period, in correlation with the compositions of the basic alloys, grouped by epochs (ancient Cu-Sn, medieval Cu-Sn-Pb, and modern Cu-Zn-Sn-Pb and Cu-Zn). These ancient processes have been kept secret by the authors (the caste effect), so they have garnered the attention of many researchers [8–12].

In authentication by technical scientific investigation, a series of archaeometric or chemometric characteristics are determined and validated with an archaeometric function.

For ancient copper-based alloy artifacts, archaeometric characteristics are the nature and distribution of allotropic phases in the base alloy and of the congruents (minerals) in the patina's thin layer structure, thickness, uniformity, and zonal colorimetry, as well as the presence and disposition of surface degradation formations (films, crusts, iridescences, bubbles, microcracks, diffusions, segregations between minerals in the patina, etc.). Among the chemometric characteristics of the alloying process, in correlation with the composition of the base alloy and the patina, the combination ratios of the main alloying components and traces are often used, for example, in the case of a modern bronze put in the process Cu/Zn, Cu/Sn, Cu/Pb, or between Cu and other microalloying elements, and in the case of a patina: O/C, O/S, O/Cl, C/S, etc. [52,53].

To compare the original artifact with the copies taken in a study, one resorts to analyzing photographic details taken under the same direction, lighting, and degree of magnification, when, in fact, one is looking at the way of arrangement of the shapes and the profile of the topographic elements in an iconographic system, the frequency of copies on the market of works of art, and their evolution over time as cultural heritage goods.

Current analyses of the few remaining samples of Greek bronzes indicate an alloy consisting of 87–88% copper and 9–10% tin, in addition to the presence of silver, iron, zinc, gold, and other metals alloyed with the base deposits. Ancient sources on bronze also indicate that lead and silver, in varying proportions, were used in alloys in the composition of statues and the process of gilding or polishing them.

It is known that the proportions of the elements that make up bronze give it a certain desired color after it has been cast. Table 2 shows the correlation between bronze composition and artifact color by Carl Dame Clark [54].

**Table 2.** Correlation between bronze composition and material color.

| Copper | Zinc | Tin | Color |
|---|---|---|---|
| 84.42 | 11.28 | 4.30 | Reddish yellow |
| 84.00 | 11.00 | 5.00 | Reddish orange |
| 83.05 | 13.03 | 3.92 | Reddish orange |
| 83.00 | 12.00 | 5.00 | Reddish orange |
| 81.05 | 15.32 | 3.63 | Reddish orange |
| 81.00 | 15.00 | 4.00 | Yellow orange |
| 78.09 | 18.47 | 3.44 | Yellow orange |
| 73.58 | 23.27 | 3.15 | Yellow orange |
| 73.00 | 23.00 | 4.00 | Pale orange |
| 70.36 | 26.88 | 2.76 | Pale yellow |
| 70.00 | 27.00 | 3.00 | Pale yellow |
| 65.95 | 31.56 | 2.49 | Pale yellow |

Table 3 shows the chronological archaeometry order of compositions for the ancient bronze artifacts [13].

**Table 3.** Evolution of elemental concentrations (%) by alloy types specific to historical periods, in chronological order.

| Type of Base Alloy | Elemental Concentration (%) | | | |
|---|---|---|---|---|
| | Cu | Sn | Pb | Zn |
| Egyptian bronze | 85.85 | 15.15 | - | - |
| Greek statuary bronze | 88.50–89.50 | 6.00–9.20 | 3.50 | - |
| Ancient Japanese and Chinese bronzes | 80.00 | 4.00 | 10.00 | 4.00 |
| Roman bronzes | 78.05–89.00 | 2.05–6.00 | 5.00 | - |
| Ancient monetary bronzes | 74.09 | 25.91 | - | - |
| Italian Renaissance bronzes | 75.00 | 25.00 | - | - |
| European Renaissance bronzes | 86.00 | 12.00 | 2.00 | - |
| French bronzes—17th century | 90.00–91.60 | 2.00–1.70 | 1.00–1.37 | 7.00–5.33 |
| French bronzes for monuments | 87.80 | 5.10 | 0.58 | 6.52 |
| Modern-age bronzes | 86.60 | 6.60 | 3.30 | 3.30 |

This work aimed to authenticate and establish the state of conservation of a bronze bust of Napoleon I, a replica of the one made in 1885 by the Italian sculptor Renzo Colombo using the lost wax casting technique, immediately followed by artificial patination, which was exhibited at the Paris Salon of Art in 1885.

In fact, due to a large number of replicas/copies made immediately after the original of 1885 was put into operation, the work focuses on the typological framing based on dimensional and structural–artistic characteristics and on the heritage value assessed based on the state of preservation and altimetric cataloging attributes [55].

The artifact was historiographically studied based on data published in some commercial catalogs of auction houses around the world, which were compared with the photographic characteristics of the physiognomy of the bust and the details of the representative areas of anthropomorphic features, clothing, inscriptions, and structural and ornamental components. Through direct analysis with magnifying instruments and indirect analysis by scanning electron microscopy (scanning) coupled with X-ray spectroscopy (SEM-EDX), the characteristics of the state of preservation and the archaeometric and chemometric characteristics of the period of commissioning were determined.

## 2. Experimental Section

### 2.1. Presentation of the Bust

The sculpture comes from a private collection. It was acquired on the open market in Corsica, France and brought to Romania in 1994. The owner is not able to provide a number of data related to the provenance, the routes traveled since the acquisition, the place, and the former owner.

The artifact was kept in the collector's living room after 1994.

The work is presumed to belong to the Italian sculptor Renzo Colombo (1856–1885) and was executed in bronze using the lost wax casting technique. It has a fine finish and a well-preserved noble patina of age. The wall thickness of the statue varies between 3 and 5 mm. The statue is of medium size, 445 mm high, 295 mm wide, 210 mm thick, weighs 14.50 kg, and is a model for display in a gallery or inside a building (Figure 1).

**Figure 1.** Image of the bust taken under gradually decreasing illumination: (**a**) front; (**b**) profile; (**c**) base.

On the left shoulder, a slightly legible inscription, representing the foundry's seal, is marked with a circular outline, painted in red (Figure 2).



**Figure 2.** Unreadable mark (**left side**) and marking area on the right shoulder (**right side**).

On the right shoulder, the author's name, "R. COLOMBO", is inscribed, and the year 1885 (Figure 3a). On the upper back on the right shoulder the variant, workshop, and place are inscribed (Figure 3b).
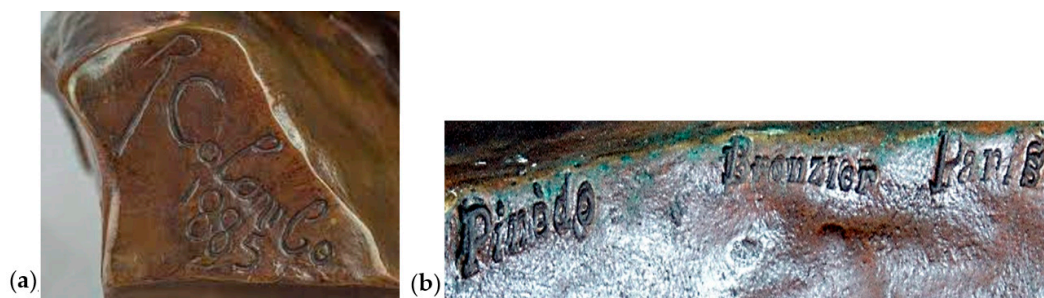


**Figure 3.** The author's inscription "RCOLOMBO" and the year 1885 on the left shoulder (**a**); the *Pinédo* variant, *Brenzier* workshop in *Paris* (**b**).

On the lower part of the bust, in front of the bust, there is a straw inscribed on a circular band on the plinth (pedestal), on the first row, reading "NAPOLEON I$^{ER}$", followed on the second row by "1812 PAR COLOMBO" (Figure 4). The pedestal is fixed to the lower part of the bust by screws hidden inside the statue (Figure 5).



**Figure 4.** The inscription on a circular band on the first row "NAPOLEON I$^{ER}$" followed on the second row by "1812 PAR COLOMBO": (**a**) original, (**b**) well-preserved replica.



**Figure 5.** The system for attaching the bowline to the lower part of the bust by a hidden screw and emphasizing the thickness of the sculpture wall: (**a**) original, (**b**) well-preserved replica.

The patina of the age of the two structural components (the statue and the eagle) denotes that they were elaborated (molded and finished) in the same period. It should be noted that the two dates inscribed on the right shoulder and the circular band under the eagle correspond to different periods: the first date on the statue is the year and the signature of the author, and the second is the year when the image of Emperor Napoleon was taken (1812). The simple, dry-stamp-like mark or seal on the right profile of the bust and the inscription on the back of the left shoulder are made by paneling before patination. After patination, the workshop mark or seal has been painted red for emphasis. While the inscription representing the maker and the year of commissioning can be found on most artifacts made after 1885 using the same casting and patination technique, very many do not bear the maker's mark, workshop, and variant.

Studying the author's life and work, as well as the catalogs of various auction houses—for example, Christie's and Sotheby's, UK; Cowan's, Cincinnati; Heritage Auctions, Dallas; Historia Auktionshaus, Berlin; Weschler's Washington; Freeman's, Philadelphia; Erich Pillon Encheres, Versailles; Schuler Auktionen, Zurich; Jackson's International Auctioneers & Appraisers, Cedar Falls; Uppsala Aucktionskammare, Uppsala; and Pook & Pook, Inc., Downingtown (Table 4)—that have appraised and marketed such statues, it was found that several replicas were made in a Parisian workshop between 1885 and 1890, a fashionable aspect at the time and well known even to the greatest sculptor of the modern world (Rodin).

**Table 4.** Appropriate models by size and structural–artistic characteristics, auction houses purchased through, date/time of sale, lot, value, and height.

| Nr. Crt. | Auction House | Date/Time of Sale | Lot | Value | Statue Size |
|---|---|---|---|---|---|
| 1. | Christie's— similar patterns, light brown patina | 31 May 2000/8369 | 171 | 9.400 USD | 21″ H |
| | | 27 November 2002/1099 | 9519 | 4700 GBP | 21 5/8″ H |
| | | 10–11 July 2002/1099 | 1099 | 4780 USD | 21 1/2″ H |
| | | 19–20 October 2011/2473 | 12 | 5.250 USD | 21 5/8″ H (Bronze Garanti au Titre cast variant). |
| | | 1 April 2003 | 766 | 2.868 USD | 31.8 cm, 12½″ H |
| | | 20 October 2011 | 1–23 | 5.530 USD | 55 cm, 21 5/8″ H |
| | | 2 December 2004 | 2162 | 1.016 USD | 19.5 cm., 7¾″ H |
| | | 22 May 1996 | 12 | 5.500 USD | 55.88 cm |
| 2. | Sotheby's, London—similar designs, yellow brown patina | 22 May 1996 | 88 | 4.800 USD | 55.88 cm |
| | | 10 May 2005/L03503 | 298 | 11,400 GBP | 22″ H (Pinédo variant) |
| | | 28 November 2006/N08232 | 52 | 5100 USD | 23″ H (Bronze Garanti au Titre cast variant) |
| | | 29 November 2006/N08233 | 53 | 4800 USD | 22″ H (Pinédo variant) |
| | | 20 April 2007/N08305 | 271 | 5400 USD | 71 cm, 28″ H |
| | | 22 April 2010/N08627 | 82 | 9375 USD | 55.9 cm, 22″ H |
| | | 2 June 2010/ | 271 | 6875 GBP | 58.5 cm, 23″ H |
| | | 1 April 2010/N08623 | 283 | 7500 USD | 22″ H |
| 3. | Cowan's, Cincinnati—dark brown patina | 11 July 2014 | 733 | - | 52.07 cm |
| | | 11 October 2014 | 893 | - | 54.61 cm |
| 4. | Heritage Auctions, Dallas—dark brown patina | 12 September 2015 | 347 | - | 55.88 cm |
| 5. | Heritage Auctions, Dallas; Historia Auktionshaus, Berlin—light brown patina | 25 February 2015 | 3803 | - | 32 cm |
| 6. | Weschler's, Washington—golden brown patina | 5 December 2015 | 163 | - | 55.88 cm |
| 7. | Freeman's, Philadelphia—gray–brown patina | 20 May 2014 | 347 | - | 55.88 × 38.1 × 27.94 cm |
| | | 26 October 2011 | 399 | - | 31.6 cm |
| 8. | Erich Pillon Encheres, Versailles—grayish brown patina | 16 March 2014 | 13 | - | 32 cm |
| 9. | Schuler Auktionen, Zurich—golden brown patina | 10 December 2012 | 3079 | - | 45 cm |
| | | 18 May 2013 | 3059 | - | 45 cm |
| 10. | Jackson's International Auctioneers & Appraisers, Cedar Falls—chocolate brown patina | 15 Nov 2011 | 322 | - | 55.5 cm |
| | | 17 July 2007 | 952 | - | 20.32 cm |
| 11. | Uppsala Aucktionskammare, Uppsala—grayish brown patina | 09 December 2001 | 258 | - | 60.96 cm |
| 12. | Pook & Pook, Inc., Downingtown—chocolate brown patina | 23 March 2007 | 58 | - | 55.88 cm |
| | | 21 November 2008 | 108 | - | 54.61 cm |
| | | 26 October 2007 | 165 | - | 31.12 cm |

Studying the trade in such statues over the last 25 years (1995–2020) through auction houses, many artifacts have been sold (Table 4), but they differ in patina hue, weight, and size. Most are chocolate brown or golden, a few dark brown or grayish brown, and in height, they range from 19.5 to 71.0 cm; most are around 55.88 cm. Of course, the same goes for weight, ranging from 14.5 to 40 kg.

Such replicas have been purchased by collectors and art galleries for between USD 400 and USD 10,498 and between GBP 4000 and GBP 11,400 respectively (according to other auction houses).

The statue, brought for examination of authenticity, state of conservation, and heritage value, is an interior bust of Napoleon Bonaparte, cast in bronze using the lost wax technique, after the 1885 model by Renzo Colombo (Italian artist, 1856–1885). The original considered a masterpiece, based on a rare marble pedestal with a cherry-tree design. Most of the children have mosaic marble pedestals or plinths, colored in grey, sepia, or green, or four wooden, postwood, leather, or non-slip polymer "buttons" (slippers), which do not damage the lacquered supporting furniture when handled.

This copy was cast in the last quarter of the 19th century. Much of Renzo Colombo's work, including numerous models of Napoleon, was executed wearing Pinédo or Bronze Garanti au Titre Cast seals. The finish and patina of this bust are typical of the Pinedo variants (as marked on the verso of the left shoulder at the top). Moreover, the work has the caster's seal applied by molding before patination, which allows for firm authentication. This model is considered a bold example, as one of Renzo Colombo's best and most popular works; in it, he portrayed Emperor Napoleon as a dignified and serious figure, with his forehead firmly extended and his eyes focused. The facial expression shows a man of intense concentration and determination, dressed in his military cloak and wearing his bicorne hat, and in front of the bust is an eagle, considered his standard, holding a double torch in its sharp talons. The scene captures Napoleon before he invaded Russia in the summer of 1812, a campaign that severely damaged the French Empire and foreshadowed the collapse of the Grande Armée. This led shortly after to Napoleon's abdication in Paris in 1814. The bust has, in addition to its original patina of red oxide–brown (a thin, continuous, and smooth film of stoneware based on oxides, chlorides, sulfides, nitrates, sulfates, and phosphates, all of which are hardly soluble, using the process of chemical precipitation by cement applied immediately after casting and finishing), one of age, in the form of vesicles; small, thin, slightly cracked crusts; and fine films with zonal distribution, especially on the prominences (tip of the nose; edges and folds of the palate and mantle).

The artist *Renzo Colombo* was born near Milan in 1856. He studied sculpture with Giuseppe Knoller, who had him as a scholarship student at the Academy of Fine Arts in Brera. During his very short life (29 years), he produced 35 sculptures considered artistic masterpieces [5–7].

Most of the models have the dimensions 15″ W × 9 1/4″ D × 21 3/4″ H (height: 56–73 cm, width: 36–41 cm, and thickness: 28–38 cm; base-to-plinth dimensions: H 17 cm; total weight: approx. 14.5–35 kg), and their condition presents as very good, with an original patina in excellent condition, with minor wear from handling and some variations in surface deterioration and decay. There are patches on the chest and back of the cap from the lost wax casting process, which has oxidized over time, making the outline visible.

## 2.2. Conservation Status

The carving is in a good state of preservation, with small iridescences, spots of corrosion (malachite), and fine scales of corrosion, and on the back, in the area of the collar and mantle, there is a fairly wide but non-invasive malachite streak, as well as on the tip of the nose and the muffs/cuts of the hat and mantle, well highlighted in Table 5 (column III, positions 4–7, 9, 10, 12–20).

The carving has four very poorly preserved screws fixed to the lower corners of the bust, for attaching buttons or slippers so as not to interfere with handling and placing on the supporting furniture (similar to a table or lapidary). These, now missing or with only stumps remaining, were threaded after casting and finishing.

The artifact is in good condition, with a well-preserved patina typical of old bronze statues. For authentication, the composition of the base alloy in the body of the artifact, as well as the patina in different areas and the screws, was analyzed. These elements align with bronze-cast artifacts from the period of 1885 to 1890. During this time, the composition of bronzes and alloys underwent significant changes due to technological and economic factors [1–4]. These, according to Table 3, when referring to French bronzes for statues from the 17th century to the modern era, contain Cu = 80.50–91.60%, Zn = 1.70–6.60, Sn = 0.60–4.50, and Pb = 3.30–7.00.

For authentication, the artifact under study's archaeometric and experimentally validated artifactometric characteristics were identified, which involved elemental compositions and stratigraphic and micro-topographic structures, which allowed for identifying the artifact's dating.

**Table 5.** Details taken of a model from the Christie's Auction House catalogs very close to the one under analysis, which were photographed at close order of magnification.

| Detail No. | Replica Presented by Christie's Auction House | Studied Replica | Detail No. | Replica Presented by Christie's Auction House | Studied Replica |
|---|---|---|---|---|---|
| 1. | | | 2. | | |
| 3. | | | 4. | | |
| 5. | | | 6. | | |
| 7. | | | 8. | | |
| 9. | | | 10. | | |
| 11. | | | 12. | | |

**Table 5.** *Cont.*

| Detail No. | Replica Presented by Christie's Auction House | Studied Replica | Detail No. | Replica Presented by Christie's Auction House | Studied Replica |
|---|---|---|---|---|---|
| 13. |  |  | 14. |  |  |
| 15. |  |  | 16. |  |  |
| 17. |  |  | 18. |  |  |
| 19. |  |  | 20. |  |  |
| 21. |  |  | 22. |  |  |
| 23. |  |  | | | |

### 2.3. Digital Imaging Methods and Techniques

The artifact was digitally photographed (using a Sony ALPHA 6000 camera, produced by Sony Technology Thailand Co., Ltd in Chonburi) from the perspective of the 5 directions of analysis (Figure 1). A series of details were photographed and compared with those of a model as close as possible to the original (Table 5, positions 1–23), which allowed for the selection of comparison systems that highlight the differences between the original and the copies.

### 2.4. Sampling and Processing of Material

According to the principles of the science of cultural heritage conservation and the wishes of the owners, the selection of the areas for sampling the material samples was made at the level of the structural elements, where the aesthetics would not be affected, using non-invasive interventions. In this sense, the sampling for the initial (artificial) and natural (old) patina was chosen from the area (A) on the left shoulder, back, where small sharp pliers were used to take the surface sample, and for the base alloy, the patina from the interior cavity of the statue and the fixing screw of the slippers or the console at the base of the statue—areas (B), (C), and (D)—were chosen from the furrow with the tail, where the sampling was performed for the surface structures with a small-pointed pliers, and for the internal ones with a drill (Figure 6).

**Figure 6.** Areas where sampling was performed: (A)—left shoulder, back; (B)—the base of the plinth (support–pedestal); (C)—the surface of the inner cavity of the statue; (D)—the bracket or statue's shoe fixing screw.

*2.5. Microscopic Methods and Techniques*

The topographic microstructure and morphology of the patinas and corrosion products were investigated by SEM-EDX technique using a scanning electron microscope, model SEM VEGA II LSH, produced by TESCAN Czech Republic (produced in Brno), coupled with an EDX detector type QUANTAX QX2, produced by BRUKER/ROENTEC Germany (Berlin). The microscope, completely computer-controlled, has an electron gun with a tungsten filament that can reach a resolution of 3 nm at 30 kV, with a magnification power between 30× and 1,000,000× in "resolution" for the mode of operation, accelerating voltage between 200 V and 30 kV, with a scanning speed between 200 ns and 10 ms per pixel. The working pressure is less than $1 \times 10^{-2}$ Pa. The image obtained can consist of secondary electrons (SE) or backscattered electrons (BSE). Quantax QX2 is an EDX detector used for qualitative and quantitative microanalysis. The EDX detector is a 3rd-generation X-flash type detector that does not require liquid nitrogen cooling and is approximately 10 times faster than conventional Si (Li) detectors. The technique, together with microphotograph visualization, allows for imaging with the mapping (arrangement) of atoms on the surface under investigation. Based on the X-ray spectrum, it is possible to determine the elemental composition (in gravimetric or atomic percentages) of a microstructure or selected area and to evaluate the composition variation along a vector arranged in the analyzed area or section [67–72].

The purpose of the diagnostic tests is related to the study of the construction technique and technology of the artifact, providing information about the original materials, their state of preservation, and the alteration products present on the artifact.

By direct analysis with magnifying instruments and indirect analysis by scanning electron microscopy with energy-dispersive X-ray spectroscopy (SEM-EDX), the characteristics of the state of preservation and the archaeometric and chemometric characteristics of the period of commissioning were determined.

**SEM-EDX analysis** [68] was performed on non-invasively sampled microprobes that had not been metallized. SEM images and EDX spectra were obtained simultaneously. Magnification ranging from 200 to 600× (in most cases selecting a 500 μm × 500 μm frame) and an integration time of 100 s were chosen. Both secondary electron (SE) and backscattered electron (BSE) mode images were acquired.

**UV, Vis, and IR reflectography** was performed using an HS525A series document detector-type device, with a USB port; 30× magnification power; UVA (365 nm), UVC (254 nm), infrared (IR), blue–white (470 nm), and laser (980 nm) fields; a 1.3 MP (2.0 MP interpolated) microscope with USB power supply with manual focus from 10 mm to 500 mm and a frame rate of max 30 f/s under 600 lx brightness; 8 white LEDs with adjustable illumination and magnification rate from 20× to 200×; AVI video format; and a portable UV illuminator (LED: G5, UV 4W).

**Optical Microscopy.** In the optical microscopy analysis, a Zeiss Imager a1M microscope was used, with an AXIOCAM camera and specialized software attached. The samples were analyzed at 50–200× magnification in a dark or bright field.

**Optical stereomicroscope. For optical stereomicroscope analysis, a** microscope type CTEPEO MX4, produced by LOMO in Saint Petersburg, to which a camera was attached, was used.

## 3. Results and Discussions

From the analysis of the data in Table 5, along with information from auction house catalogs, it can be concluded that after 1885, a large series of busts of Napoleon was produced. These busts were created using the lost wax casting technique, followed by finishing, artificial patination, and transparent coating. While many are similar in model and statuary style, there are notable differences in material (bronze, brass, or marble), patinas (ranging from golden brown, reddish brown, dark brown, and light brown to grayish and grayish-black), as well as in structural and dimensional aspects. These variations include differences in clothing, head and eagle positions and orientations, and size and weight. Thus, in comparison with most bronze busts, the artifact under study shows very few differences in pattern, easily evident in all 23 comparative details in Table 5.

*SEM-EDX Analysis*

Figures 7–9 show the SEM microphotographs at one or two degrees of magnification, used in the comparative analysis of the different samples taken from the areas shown in Figure 6 both from the surface (Figure 6, A and B) and from the interior cavity of the statue (Figure 6, C), which did not affect the aesthetics of the artefact, and, respectively, from a screw (Figure 6, D), for fixing by threading into the base or into cuffs made of non-stick material that do not leave scratch marks on the display surface.
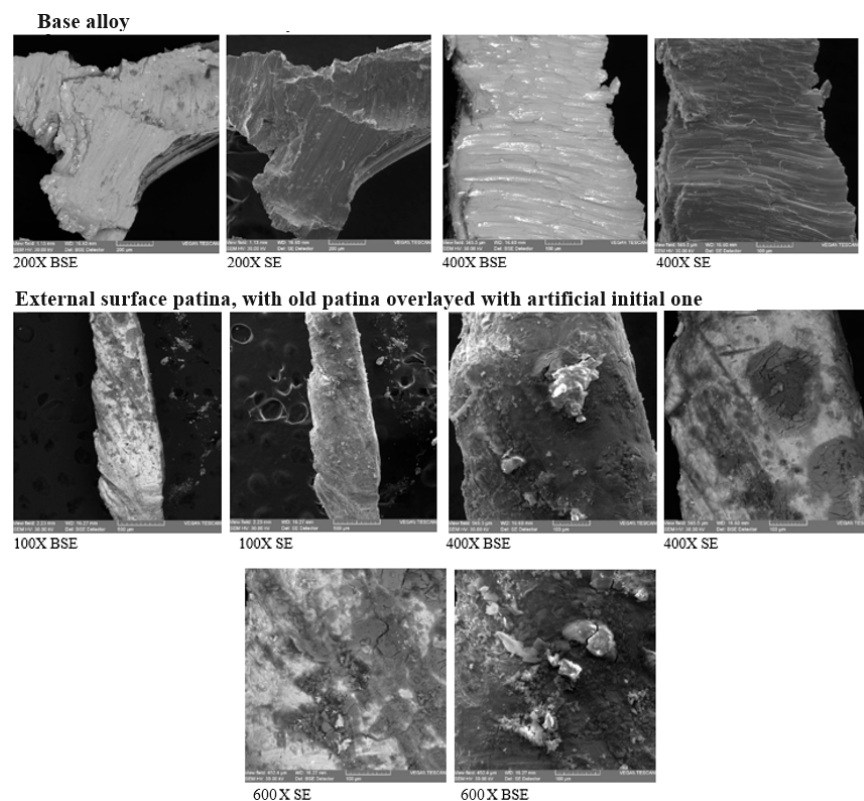


**Figure 7.** SEM photomicrographs of the base alloy in Area B of the plinth and the two patinas in Area A from the surface of the left-rear shoulder of the statue (non-invasive microsampling) seen in Figure 6.
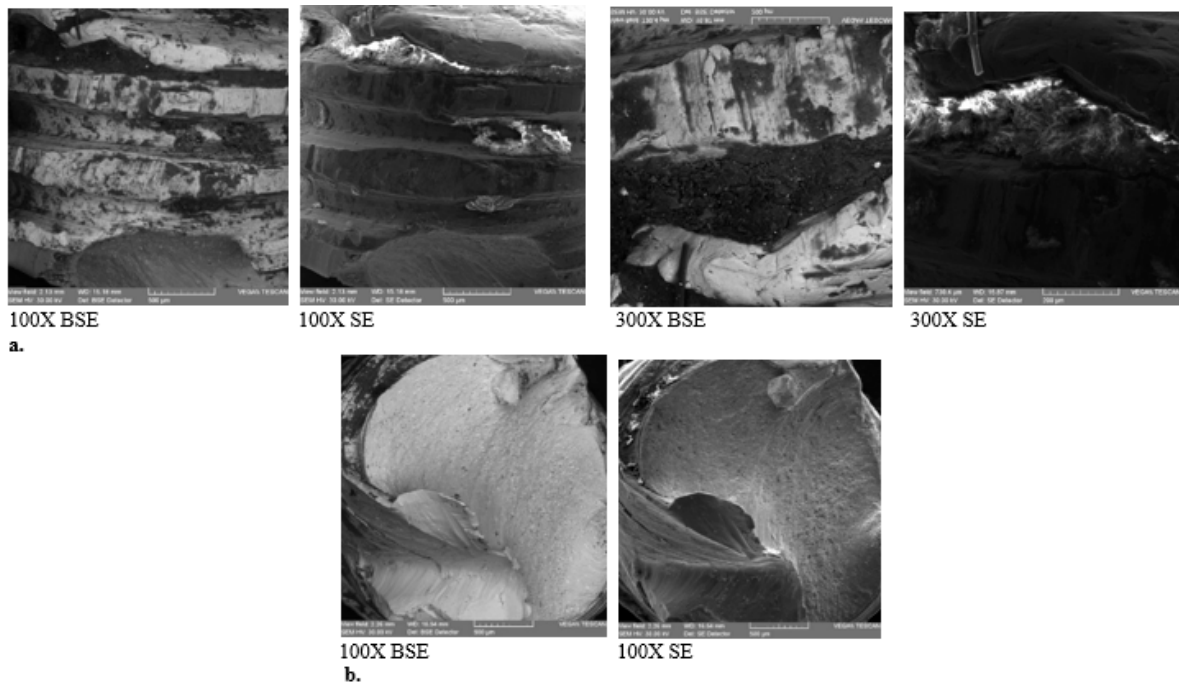
**Figure 8.** SEM microphotographs of the fixing screw of the console at the base of the statue (area in Figure 6, D): (**a**) lateral surface and (**b**) transverse surface in fresh cutting.
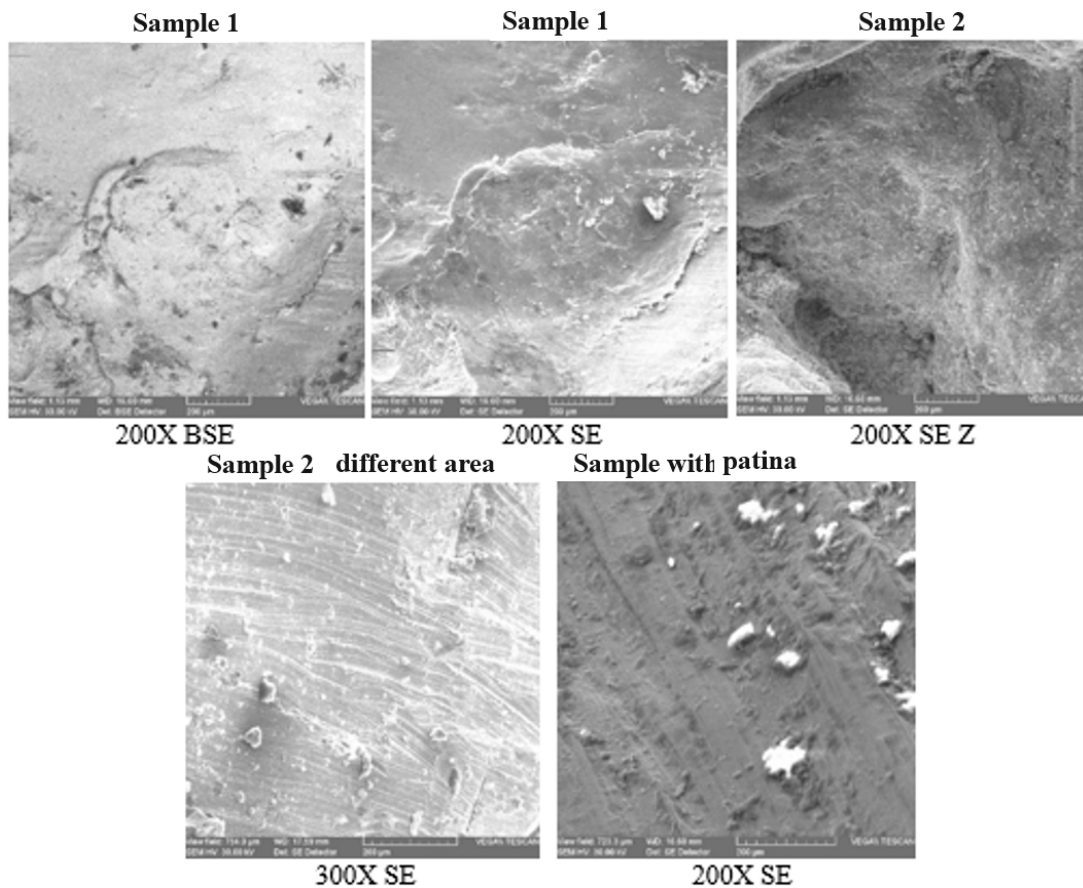


**Figure 9.** SEM microphotographs on the surface of the inner cavity of the statue (area in Figure 6, C).

The purpose of taking a sample of one of the four screws fixing the console at the base of the statue was to check whether it was cast in wax lost with the statue, after which

the thread was made, or whether it is made of another threadable bronze- or brass-based material.

The analysis of SEM micrographs shows the homogeneity of the alloy, the roughness of the initial or resulting surfaces at cutting for sampling, and the crystallites/granulites in the fresh-cut and time patina areas, which allows for evaluation of the processes of artifact development/turning and sampling. Initially, as shown in Figures 7–9, SEM-EDX analyses were performed on samples taken from several areas, and after processing, only the most representative samples with well-defined compositions were retained in this study.

Figure 10 is presented as an example: EDX spectra with the analyzed area, previously determined by OM, of samples taken from the freshly cut surface of the alloy and of the artificial patina obtained at the in-service, after lost wax casting, followed by microburr and surface finishing. Similar analysis was carried out for each sample/area, as summarized in Table 6 (voltage of SEM was set to 20 kV).
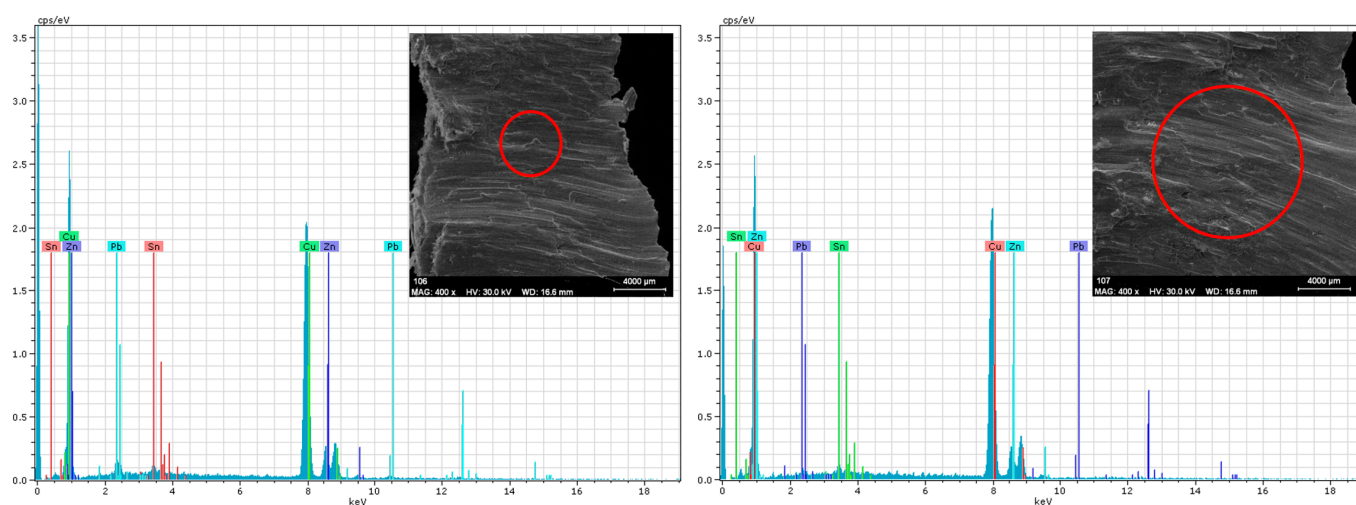


**Figure 10.** EDX spectrum of the base alloy from two central sample areas—400× BSE and 500× SE.

**Table 6.** Elemental (%), gravimetric (Wt), and atomic (At) composition of non-invasively extracted microsamples taken from the external surface of the statue.

| Sample | Chemical Element | X-ray Spectra | Normal Wt (%) | Normal At (%) | Error (%) |
|---|---|---|---|---|---|
| S1 (zone 123, 400× SE, central base alloy, area in Figure 6, B) | Copper | Series-K | 75.695 | 82.484 | 2.444 |
| | Zinc | Series-K | 11.814 | 12.511 | 0.488 |
| | Tin | Series-K | 3.333 | 1.944 | 0.383 |
| | Lead | Series-K | 9.156 | 3.060 | 0.521 |
| | Total | | 100 | 100 | |
| S2 (zone 124, 400× SE, bottom base alloy, area in Figure 6, D) | Copper | Series-K | 77.196 | 83.348 | 2.445 |
| | Zinc | Series-K | 11.521 | 12.089 | 0.484 |
| | Tin | Series-K | 3.347 | 1.934 | 0.368 |
| | Lead | Series-K | 7.933 | 2.627 | 0.503 |
| | Total | | 100 | 100 | |
| S3 (zone 125, 200× central base alloy, area in Figure 6, B) | Copper | Series-K | 71.382 | 80.503 | 2.238 |
| | Zinc | Series-K | 11.235 | 12.314 | 0.501 |
| | Tin | Series-K | 4.539 | 2.740 | 0.708 |
| | Lead | Series-K | 12.841 | 4.441 | 0.776 |
| | Total | | 100 | 100 | |

**Table 6.** *Cont.*

| Sample | Chemical Element | X-ray Spectra | Normal Wt (%) | Normal At (%) | Error (%) |
|---|---|---|---|---|---|
| S4 (zone 118, center patina up, area in Figure 6, C) | Copper | Series-K | 42.000 | 19.406 | 1.196 |
| | Zinc | Series-K | 6.674 | 2.997 | 0.240 |
| | Lead | Series-K | 4.092 | 0.579 | 0.212 |
| | Tin | Series-K | 3.562 | 0.881 | 0.239 |
| | Iron | K-series | 0.488 | 0.256 | 0.052 |
| | Calcium | K-series | 0.095 | 0.069 | 0.034 |
| | Sodium | K-series | 7.049 | 9.003 | 4.648 |
| | Aluminum | K-series | 0.334 | 0.363 | 0.062 |
| | Silicon | K-series | 0.302 | 0.316 | 0.054 |
| | Carbon | K-series | 4.487 | 10.970 | 2.337 |
| | Sulfur | K-series | 0.851 | 0.779 | 0.093 |
| | Chlorine | K-series | 0.725 | 0.600 | 0.070 |
| | Phosphorus | K-series | 0.064 | 0.060 | 0.036 |
| | Oxygen | K-series | 29.269 | 53.713 | 5.054 |
| | Total | | 100 | 100 | |
| S5 (zone 119, center patina top right, area in Figure 6, A) | Copper | Series-K | 52.859 | 27.661 | 1.658 |
| | Zinc | Series-K | 8.381 | 4.261 | 0.333 |
| | Lead | Series-K | 4.809 | 0.771 | 0.291 |
| | Tin | Series-K | 2.789 | 0.781 | 0.220 |
| | Iron | K-series | 0.449 | 0.267 | 0.058 |
| | Calcium | K-series | 0.049 | 0.041 | 0.033 |
| | Aluminum | K-series | 0.169 | 0.208 | 0.056 |
| | Silicon | K-series | 0.213 | 0.252 | 0.055 |
| | Carbon | K-series | 5.894 | 16.320 | 3.128 |
| | Sulfur | K-series | 0.463 | 0.480 | 0.078 |
| | Chlorine | K-series | 0.597 | 0.560 | 0.075 |
| | Phosphorus | K-series | 0.082 | 0.088 | 0.040 |
| | Oxygen | K-series | 23.239 | 48.302 | 5.185 |
| | Total | | 100 | 100 | |
| S6 (zone 120, central crust patina, mobile, area in Figure 6, A) | Copper | Series-K | 33.718 | 13.682 | 1.042 |
| | Zinc | Series-K | 5.678 | 2.239 | 0.220 |
| | Lead | Series-K | 3.951 | 0.491 | 0.208 |
| | Tin | Series-K | 3.119 | 0.677 | 0.191 |
| | Sodium | K-series | 8.315 | 9.326 | 5.303 |
| | Aluminum | Series-K | 0.653 | 0.624 | 0.084 |
| | Carbon | K-series | 5.732 | 12.307 | 1.588 |
| | Sulfur | K-series | 1.287 | 1.035 | 0.108 |
| | Chlorine | Series-K | 0.762 | 0.554 | 0.071 |
| | Phosphorus | Series-K | 0.276 | 0.230 | 0.058 |
| | Oxygen | Series-K | 36.504 | 58.831 | 6.049 |
| | Total | | 100 | 100 | |

| Sample | Chemical Element | X-ray Spectra | Normal Wt (%) | Normal At (%) | Error (%) |
|---|---|---|---|---|---|
| S7 (zone 121, mobile crystallites, agglomerates, area in Figure 6, A) | Copper | Series-K | 33.683 | 14.116 | 1.110 |
| | Zinc | Series-K | 5.490 | 2.236 | 0.242 |
| | Tin | Series-K | 4.672 | 1.048 | 0.355 |
| | Lead | Series-K | 5.508 | 0.707 | 0.311 |
| | Iron | Series-K | 0.674 | 0.321 | 0.065 |
| | Chrome | Series-K | 0.332 | 0.170 | 0.050 |
| | Calcium | Series-K | 0.132 | 0.087 | 0.039 |
| | Magnesium | Series-K | 0.672 | 0.736 | 0.114 |
| | Aluminum | Series-K | 1.259 | 1.243 | 0.139 |
| | Silicon | Series-K | 1.124 | 1.066 | 0.114 |
| | Carbon | K-series | 6.494 | 14.399 | 2.342 |
| | Sulfur | K-series | 1.376 | 1.142 | 0.130 |
| | Chlorine | Series-K | 1.226 | 0.921 | 0.105 |
| | Phosphorus | Series-K | 0.464 | 0.399 | 0.069 |
| | Oxygen | Series-K | 36.888 | 61.402 | 8.730 |
| | Total | | 100 | 100 | |
| S8 (zone 122, 400× BSE, central patina crystallite, area in Figure 6, A) | Copper | Series-K | 38.915 | 17.185 | 1.239 |
| | Zinc | Series-K | 5.583 | 2.396 | 0.241 |
| | Tin | Series-K | 2.952 | 0.697 | 0.274 |
| | Lead | Series-K | 4.132 | 0.559 | 0.254 |
| | Iron | Series-K | 0.305 | 0.153 | 0.050 |
| | Sodium | Series-K | 9.007 | 10.995 | 6.835 |
| | Magnesium | Series-K | 0.211 | 0.108 | 0.045 |
| | Calcium | Series-K | 0.109 | 0.076 | 0.038 |
| | Aluminum | Series-K | 0.791 | 0.823 | 0.108 |
| | Silicon | Series-K | 0.424 | 0.424 | 0.070 |
| | Carbon | K-series | 4.402 | 10.285 | 1.866 |
| | Sulfur | K-series | 0.743 | 0.650 | 0.095 |
| | Phosphorus | Series-K | 0.178 | 0.162 | 0.051 |
| | Chlorine | Series-K | 1.108 | 0.877 | 0.099 |
| | Oxygen | Series-K | 31.132 | 54.604 | 5.881 |
| | Total | | 100 | 100 | |
| S9 (zone 127, screw, external thread 100× coated, area in Figure 6, D) | Copper | Series-K | 49.719 | 24.426 | 1.549 |
| | Zinc | Series-K | 7.597 | 3.627 | 0.308 |
| | Tin | Series-K | 2.524 | 0.664 | 0.179 |
| | Lead | Series-K | 4.120 | 0.620 | 0.267 |
| | Iron | Series-K | 0.480 | 0.268 | 0.059 |
| | Aluminum | Series-K | 0.961 | 1.112 | 0.128 |
| | Silicon | Series-K | 2.920 | 3.246 | 0.228 |
| | Carbon | Series-K | 8.308 | 21.595 | 2.864 |
| | Phosphorus | Series-K | 0.142 | 0.143 | 0.049 |
| | Sulfur | Series-K | 0.485 | 0.472 | 0.086 |
| | Chlorine | Series-K | 0.508 | 0.447 | 0.077 |
| | Oxygen | Series-K | 22.228 | 43.373 | 5.230 |
| | Total | | 100 | 100 | |

**Table 6.** *Cont.*

| Sample | Chemical Element | X-ray Spectra | Normal Wt (%) | Normal At (%) | Error (%) |
|---|---|---|---|---|---|
| S10<br>(zone 128, screw with thread recess deposition, 100×, area in Figure 6, D) | Copper | Series-K | 2.362 | 0.893 | 0.188 |
| | Zinc | Series-K | 4.012 | 1.517 | 0.315 |
| | Tin | Series-K | 5.146 | 1.072 | 0.904 |
| | Lead | Series-K | 6.626 | 0.791 | 0.591 |
| | Iron | Series-K | 10.355 | 4.587 | 0.514 |
| | Calcium | Series-K | 0.840 | 0.518 | 0.638 |
| | Magnesium | Series-K | 0.898 | 0.914 | 0.190 |
| | Bariu | Series-K | 9.445 | 1.701 | 0.528 |
| | Aluminum | Series-K | 3.565 | 3.269 | 0.378 |
| | Silicon | Series-K | 7.873 | 6.934 | 0.599 |
| | Carbon | Series-K | 7.696 | 15.851 | 3.899 |
| | Sulfur | Series-K | 3.072 | 2.370 | 0.381 |
| | Phosphorus | Series-K | 0.351 | 0.281 | 0.087 |
| | Oxygen | Series-K | 38.529 | 59.572 | 10.680 |
| | | Total | 100 | 100 | |
| S11<br>(zone 129, thread recess deposition, 300×, area in Figure 6, D) | Copper | Series-K | 5.850 | 2.434 | 0.346 |
| | Zinc | Series-K | 2.306 | 0.932 | 0.221 |
| | Tin | Series-K | 8.595 | 1.914 | 1.024 |
| | Lead | Series-K | 13.646 | 1.741 | 0.895 |
| | Iron | Series-K | 3.577 | 1.693 | 0.235 |
| | Calcium | Series-K | 3.774 | 2.490 | 1.202 |
| | Potassium | Series-K | 1.557 | 1.053 | 0.166 |
| | Magnesium | Series-K | 1.445 | 1.572 | 0.203 |
| | Aluminum | Series-K | 4.000 | 3.920 | 0.327 |
| | Silicon | Series-K | 11.275 | 10.615 | 0.632 |
| | Carbon | Series-K | 5.812 | 12.793 | 9.390 |
| | Sulfur | Series-K | 2.285 | 1.884 | 0.224 |
| | Chlorine | Series-K | 1.408 | 1.050 | 0.170 |
| | Phosphorus | Series-K | 1.312 | 1.120 | 0.145 |
| | Oxygen | Series-K | 33.151 | 54.783 | 17.017 |
| | | Total | 100 | 100 | |

Table 6 shows the elemental composition in mass and atomic percentages.

In this case, we can see the three chemical element groups: those of the base alloy (Cu, Zn, Pb, and Sn), written/notated in black; those of the initial artificial patina, superimposed on the natural aged patina (Fe, Ca, Mg, Na, Ba, Al, Si, C, S, Cl, and P), written/notated in blue; and oxygen, separately written in red. These were found in most congruents of both the initial and the naturally aged patina, as well as in the deposits of anchor dirt formed during the ageing process under the influence of microclimatic agents (in particular humidity, temperature, and light), chemical agents (atmospheric oxygen, carbon dioxide, other acid anhydrides, ammonia, tar, oils, saliva splashes, insect and bird dirt, etc.), and microbiological (fungi, yeasts, etc.), along with atmospheric dust and smog.

For sample S4, taken from a central area, with a uniform patina, the error in determining the composition of oxygen is over 5.000, along with copper at 1.196, sodium at 4.648, and carbon at 2.337; the remaining elements have errors below 0.240, down to a minimum of 0.034 (a single stable chemical compound, but with a non-uniform distribution, is rarely observed). Further, the last chemical elements, which have errors below 0.240, form a single congruent, whereas carbon is found in the composition of two (S4), four (S10), and even nine (S11) congruents, of the carbonate type, and sodium in four congruents of the chloride, sulfide, sulfate, and phosphate type. Oxygen, in the first case (S4), is found in the form of oxides, carbonates, sulfates, phosphates, oxo- and hydroxocomplexes and aluminosilicates. In the second case (S10), along with the last ones, the diversity of compounds also increases through the formation of allotropic structures. The third case (S11), in addition to those presented above, was found in oxidatively anchored surface structures and those in the form of clusters, with non-uniform zonal distributions. This is a notorious case for such a large, almost inadmissible error of 17.017, which is put down to a very large number of oxidic, sulfhydric, hydroxocomplex, oxosharing compounds both for the four alloying elements (Cu, Zn, Pb, and Sn) and for the artificial/natural patination and contamination (aluminosilicates, calcium carbonate, and sulfate—chalk dust and gypsum).

This way of separating the chemical elements into the three groups allowed for the evaluation of the chemical nature of the structural components and their 3D distribution in a cross-section and planimetric 3D.

Experimentally validated archaeometric (Table 7) and chemometric characteristics identified by high-resolution OM and Stereomicroscopy SMO in conjunction with SEM-EDX electron microscopy were also processed for reliable quantification.

**Table 7.** Elemental composition of the main and microalloying components of the base alloy used in the evaluation as validated archaeometric ratios by EDX elemental analysis.

| Sample | Main Alloy Components | | | |
|---|---|---|---|---|
| | Cu (%) | Zn (%) | Sn (%) | Pb (%) |
| S1 (freshly cut area with homogeneous surface) | 49.44 */25.00 ** | 9.38 */4.60 ** | 2.45 */0.66 ** | 5.13 */0.79 ** |
| S2 (freshly cut area with non-homogeneous surface) | 54.28 */32.44 ** | 4.43 */2.57 ** | 3.28 */1.05 ** | 10.54 */1.93 ** |
| S3 (freshly cut area) | 74.15 */76.87 ** | 10.79 */10.87 ** | 3.55 */2.00 ** | 7.62 */2.42 ** |
| S4 (old patina area) | 33.67 */12.92 ** | 5.74 */2.14 ** | 3.32 */0.68 ** | 2.88 */0.34 ** |

*—maximum concentration limit. **—minimum concentration limit.

Except for samples S1, S2, S3, and S6, the others show in the composition of the surface the elements iron, phosphorus, chlorine, and carbon, which shows that the patina is artificial and not natural.

Based on the data in Table 3, the chemometric characteristics (composition ratios of the main alloy components) were obtained, which were then correlated with those calculated for the alloy groups specific to the four periods evaluated by approximate framing of the data in Table 7:

Renaissance bronzes: Cu/Sn/Pb = 43/6/1;
Seventeenth-century French bronzes: Cu/Zn/Sn/Pb = 90/6/2/1;
French monumental bronzes: Cu/Zn/Sn/Pb = 88/6/5/1;
Modern-age bronzes: Cu/Zn/Sn/Sn/Pb = 87/3/3/7/3.

Among the archaeometric characteristics, the homogeneity of the alloy, the roughness of the initial or polished surfaces, the distribution of the aged patina, and the degree of its penetration into the initial artificial patina, the extension of the erosion zones by handling and display/storage were studied by analyzing the morphology of crystallites/granulites on the surface of the old patina, typology of microcracks in the two patinas, differences in clothing (shape and its components), and biometrics compared to known and rigorously authenticated models (through ownership, donation, transfer documents, etc., or by expert reports).

For metal artifacts, the framing within the period of commissioning an archaeometric feature is accomplished by validating the composition ratios of the primary and secondary (microalloying) components of the base alloy.

The chemometric ratio with approximate evaluation for S1 is Cu/Zn/Sn/Pb = 50/9/3/5, for S2 is Cu/Zn/Sn/Pb = 55/4/3/11, for S3 is Cu/Zn/Sn/Pb = 38/5/2/4, and for S4 is Cu/Zn/Sn/Pb = 11/2/1/1, which is close to the composition of modern period bronzes. The shifts towards somewhat different archaeometric ratios is put down to the sampling areas, affected by much different values of microclimatic parameters.

For a better evaluation of all the structural elements, one of the four screws fixing the knobs or soles at the base of the statue was analyzed, with the role of eliminating iridescence/scratches on the surface of the console or furniture support during handling/placement (Figure 5a), as well as some areas inside the statue and patinated surfaces (Figure 5b), shown in Table 8 (areas on the screws) and Table 9 (areas inside the statue).

**Table 8.** Elemental composition (%) EDX gravimetric (Wt) and atomic (At) EDX of the screw holding the console statue.

| Sample | Chemical Element | X-ray Spectra | Normal Wt (%) | Normal At (%) | Error (%) |
|---|---|---|---|---|---|
| S1<br>(central zone,<br>cross-section, area in Figure 6, D) | Copper | Series-K | 80.532 | 85.093 | 2.614 |
| | Zinc | Series-K | 11.900 | 12.220 | 0.471 |
| | Tin | Series-K | 0.970 | 0.549 | 0.142 |
| | Lead | Series-K | 6.597 | 2.138 | 0.404 |
| | | Total | 100 | 100 | |
| S2<br>(marginal zone, cross-section, area in Figure 6, D) | Copper | Series-K | 77.589 | 83.710 | 2.746 |
| | Zinc | Series-K | 11.762 | 12.333 | 0.617 |
| | Tin | Series-K | 1.753 | 1.013 | 0.454 |
| | Lead | Series-K | 8.896 | 2.944 | 0.722 |
| | | Total | 100 | 100 | |

The screw concentration data show that the screw was cast with the statue, and the thread was made after artificial patination. The composition of the thread is very close to that of the body of the statue, but there are small differences due to surface contamination.

The four samples S1–S4 were analyzed using EDX from different areas inside the statue and showed concentration data appropriate to the samples taken from areas on the surface of the statue. The differences are due, on the one hand, to the cryptoclimate inside the statue, which better preserved the original artificial patina, and on the other hand, to the different patination treatment inside the statue compared to the outside.

Among the archaeometric characteristics, the homogeneity of the alloy, the roughness of the initial or polished surfaces, the distribution of the aged patina and the degree of its penetration into the initial artificial patina, and the extension of the erosion zones by handling and display/storage were studied by OM, and SOM was used to assess the morphology of crystallites/granulites on the surface of the old patina, the typology of microcracks in the two patinas, the differences in clothing (shape and its components), and biometrics compared to known and rigorously authenticated models (through ownership documents, donation, transfer, etc., or by expert reports).

**Table 9.** Elemental (%), gravimetric (Wt), and atomic (At) composition samples taken from the surfaces inside the statue.

| Sample | Chemical Element | X-ray Spectra | Normal Wt (%) | Normal At (%) | Error (%) |
|---|---|---|---|---|---|
| S1 (cleaned area, Figure 6, C) | Copper | Series-K | 49.436 | 24.975 | 2.049 |
| | Zinc | Series-K | 9.376 | 4.603 | 0.512 |
| | Tin | Series-K | 2.451 | 0.663 | 0.350 |
| | Lead | Series-K | 5.125 | 0.794 | 0.474 |
| | Iron | Series-K | 2.227 | 1.280 | 0.170 |
| | Aluminum | Series-K | 2.260 | 2.688 | 0.332 |
| | Silicon | Series-K | 1.326 | 1.516 | 0.203 |
| | Carbon | Series-K | 11.565 | 30.910 | 4.129 |
| | Oxygen | Series-K | 16.234 | 32.571 | 6.200 |
| | | Total | 100 | 100 | |
| S2 (unfinished area, Figure 6, C) | Copper | Series-K | 54.282 | 32.441 | 2.054 |
| | Zinc | Series-K | 4.420 | 2.567 | 0.339 |
| | Tin | Series-K | 3.277 | 1.048 | 0.449 |
| | Lead | Series-K | 10.544 | 1.933 | 0.799 |
| | Iron | Series-K | 0.963 | 0.655 | 0.131 |
| | Silicon | Series-K | 2.549 | 3.447 | 0.311 |
| | Aluminum | Series-K | 2.150 | 3.026 | 0.328 |
| | Carbon | Series-K | 3.933 | 12.435 | 2.434 |
| | Oxygen | Series-K | 17.882 | 42.448 | 6.716 |
| | | Total | 100 | 100 | |
| S3 (rough area, Figure 6, C) | Copper | Series-K | 74.146 | 76.869 | 2.169 |
| | Zinc | Series-K | 10.788 | 10.868 | 0.388 |
| | Tin | Series-K | 3.545 | 1.968 | 0.315 |
| | Lead | Series-K | 7.606 | 2.418 | 0.378 |
| | Iron | Series-K | 1.119 | 1.320 | 0.082 |
| | Silicon | Series-K | 2.796 | 6.557 | 0.215 |
| | Oxygen | | | | |
| | | Total | 100 | 100 | |
| S4 (patina, Figure 6, C) | Copper | Series-K | 33.670 | 12.921 | 1.133 |
| | Zinc | Series-K | 5.741 | 2.141 | 0.230 |
| | Tin | Series-K | 3.316 | 0.681 | 0.194 |
| | Lead | Series-K | 2.880 | 0.339 | 0.163 |
| | Iron | Series-K | 0.552 | 0.241 | 0.052 |
| | Carbon | Series-K | 10.750 | 21.825 | 2.503 |
| | Silicon | Series-K | 2.268 | 1.969 | 0.171 |
| | Aluminum | Series-K | 2.178 | 1.969 | 0.187 |
| | Phosphorus | Series-K | 0.559 | 0.440 | 0.066 |
| | Chlorine | Series-K | 0.687 | 0.472 | 0.067 |
| | Oxygen | Series-K | 37.399 | 57.002 | 6.654 |
| | | Total | 100 | 100 | |

For metal artifacts, a commonly used archaeometric feature for the period of commissioning is the validation of the composition ratios of the primary and secondary (microalloying) components of the base alloy.

## 4. Conclusions

This paper details the authentication analysis of a bronze bust of Napoleon I, attributed to the Italian artist Renzo Colombo (1856–1885). The bust was created using the lost wax technique and artificially patinated through a chemical hot-curing process in the Pinédo variant, in the Brenzier studio in Paris. The piece bears Colombo's signature and other casting and molding inscriptions, linking it to his known works.

Historiographical analysis, including of the specialized literature and auction house catalogs, was employed alongside comparative studies (altimetry) of photographs capturing key features of the bust, such as the anthropomorphic details, clothing, inscriptions, and ornamental components. The bust was further examined through direct analysis with magnifying instruments and indirect analysis via scanning electron microscopy coupled with energy-dispersive X-ray spectroscopy (SEM-EDX). These methods provided insight into the bust's state of preservation, its material composition, and the period of its creation. Notably, special attention was given to the evaluation of chemical congruence and errors in the EDX atomic composition, which is a critical tool in determining the authenticity of such works.

Based on the gathered data, it was concluded that the bust is a faithful replica of the original bronze bust exhibited by Colombo at the 1885 Paris Art Salon. The work was likely produced around $1890 \pm 3$, as indicated by the condition of the base alloy and the two patinas: the artificial patina applied immediately after casting and the natural patina that developed over time. This careful examination places the bust within the late 19th century, shortly after the creation of the original.

The bust itself presents Napoleon as a dignified and serious figure, wearing a military cloak and bicorne hat. His face reflects intense concentration and determination, while an eagle, symbolizing his personal standard, clutches a double torch at the front of the bust. This scene portrays Napoleon prior to his ill-fated Russian campaign in 1812, a turning point that led to the decline of the French Empire and his eventual abdication in 1814.

The bust exhibits two distinct layers of patina: an original brown-waxy patina and a reddish-brown stoneware layer formed through chemical precipitation. This latter patina, which includes oxides, chlorides, sulfides, and other compounds, was applied immediately after casting and has aged naturally, resulting in small blisters, fine films of corrosion, and areas of wear, particularly on prominent features like the nose, cheekbones, and folds of the cloak.

The patina on both the statue and the eagle indicates they were crafted and finished in the same period. Additionally, two inscribed dates on the bust—one representing the author's signature and the year of its commission, and the other marking the year of Napoleon's 1812 campaign—align with known historical details. The maker's mark and workshop seal were applied before patination, with the seal later highlighted in red. These details are consistent with other works by Colombo from this era, which often feature similar marks but sometimes lack the workshop or maker's signature.

The bust bears the Pinédo and Bronze Garanti Garanti au Titre Cast seals, typical of Colombo's works, further confirming its authenticity. The finish and patina are characteristic of the Pinédo variant, with the workshop's seal applied through die-casting before patination, which supports its firm authentication as a genuine work from the period.

**Author Contributions:** Conceptualization, methodology, and supervision, I.S.; conceptualization, investigation, data curation, and visualization, A.D., A.V.S., and V.V.; conceptualization, original draft preparation, resources, and formal analysis, V.D., C.T.I., and I.G.S. All authors have read and agreed to the published version of the manuscript.

**Institutional Review Board Statement:** Not applicable.

**Informed Consent Statement:** Not applicable.

**Data Availability Statement:** The required data is presented within the article.

# References

1. Sandu, I.; Cotiuga, V. *Cercetarea Bunurilor de Patrimoniu Şi a Documentelor Falsificate*; AIT Laboratory: Bucuresti, Romania, 2011.
2. Sandu, I.; Vasilache, V. *Conservarea Amprentelor Formă Şi a Urmelor Materiale*; AIT Laboratory: Bucuresti, Romania, 2011.
3. Matei, G. *Investigarea Criminalistică a Infracţiunilor Privind Operele de Artă Şi Artefactele Arheologice*; Universul Juridic: Bucuresti, Romania, 2019.
4. Baker, P. *Protecting Art, Protecting Artists and Protecting Consumers Conference*; Autralian Institute of Criminology: Sydney, Australia, 1999.
5. Arnau, F. *Arta Falsificatorilor—Falsificatorii Artei (in Romanian)*; Meridiane: Bucuresti, Romania, 1970.
6. Sandu, I.C.A.; Sandu, I.; Popoiu, P.; Van Saanen, A. *Aspecte Metodologice Privind Conservarea Ştiinţifică a Patrimoniului Cutural*; Corson: Iaşi, Romania, 2001.
7. Sandu, I.; Sandu, I.C.A.; Van Saanen, A. *Expertiza Ştiinţifică a Operelor de Artă*; Universităţii Alexandru Ioan Cuza: Iaşi, Romania, 1998.
8. Sandu, I. *Degradarea Şi Deteriorarea Bunurilor de Patrimoniu Cultural, Vol. I. Bunuri Din Material Anorganice*; Universităţii Alexandru Ioan Cuza: Iaşi, Romania, 2008.
9. Sandu, I.; Dima, A.; Sandu, I.G. *Restaurarea Şi Conservarea Artefactelor Metalice*; Corson: Iaşi, Romania, 2002; p. 666.
10. Sandu, I. New Materials and Advanced Procedures of Conservation Ancient Artifacts. *Appl. Sci.* **2023**, *13*, 8387. [CrossRef]
11. Sandu, I. Modern Aspects Regarding the Conservation of Cultural Heritage Artifacts. *Int. J. Conserv. Sci.* **2022**, *13*, 1187–1208.
12. Sandu, I.G.; Sandu, I.; Dima, A. *Aspecte Moderne Privind Conservarea Patrimoniului Cultural, Vol. III. Autentificarea Şi Restaurarea Artefactelor Din Materiale Anorganice*; Performantica: Iaşi, Romania, 2006; p. 502.
13. Dumitrescu, E. *Artă Si Tehnologie: Sculptura în Bronz—Despre Turnarea Formelor Prin Metoda Cerii Pierdute*; UNARTE: Bucuresti, Romania, 2010; pp. 93–98.
14. Kjellberg, P. *Bronzes of the Nineteenth Century: Dictionary of Sculptors*, Early ed.; Schiffer Publishing Ltd.: Atglen, PA, USA, 1994; p. 684. ISBN 0887406297/9780887406294 (a se vedea pagina 220).
15. Lami, S. *Dictionnaire des Sculpteurs de L'École Français, Au Dix-Neuvième Siècle, Vol. I*; Hachette Livre–BNF: Paris, France, 1970; p. 85.
16. de Champeaux, A. *Dictionnaire des Fondeurs, Ciseleurs, Modelleurs en Bronze, et Doreurs, Vol. I*; Rouam, J., Ed.; Librairie de l'Art: Paris, France, 1886; p. 357.
17. Stanley, C. *The Technique of Early Greek Sculpture*; Oxford at Clarendon Press: London, UK, 1933.
18. Dame, C.C. *Metal Casting of Sculpture*; The Standard Arts Press: Butler, MD, USA, 1948.
19. Edilberto, F. *I Grandi Bronzi Antichi—Le Fonderie e le Tecniche Di Lavorazione Dall'eta Arcaica al Rinascimento*; Nuova Imagine Editrice: Siena, Italy, 1999.
20. Gallardo, J.M.; Cuevas, F.G.; Cintas, J.; Montes, J.M. La Fe Victoriosa Casting Features. *Adv. Mater. Forum* **2008**, *587–588*, 1014–1018. [CrossRef]
21. Castelle, M.; Bormand, M.; Vandenberghe, Y.; Bourgarit, D. Two of a Kind: Shining New Light on Bronze Spiritelli Attributed to Donatello. *Stud. Conserv.* **2000**, *65*, 200–211. [CrossRef]
22. Castelle, M.; Coquinot, Y.; Bourgarit, D. Casting cores of French bronze statues of the 16th and 17th centuries: Identification of regional practices and artistic choices. *Microchem. J.* **2016**, *126*, 121–131. [CrossRef]
23. Agnoletti, S.; Brini, A.; Cagnini, A. Le Teste in Bronzo Della Cantoria Di Donatello: Aspetti Conoscitivi e Conservativi. *OPD Restaur.* **2013**, *25*, 201–212.
24. Ammannatti, N.; Paita, A.; Toni, S. *Analisi Morfologica e Composizionale di Frammenti Metallici Provenienti dal Monumento Equestre di Cosimo I*; CR Europa Metalli Rapporto: Fornaci di Barga, Italy, 1993; No. 930507/0647.
25. Bassett, J.; Scherf, G. Jean-Antoine Houdon: Sculptor and founder. In *French Bronze Sculpture: Materials and Techniques 16th–18th Century*; Archetype: Paris, France, 2014; pp. 107–124.
26. Bourgarit, D.; Bewer, F.G.; Bresc-Bautier, G. Francesco Bordoni: Specificites techniques chez un fondeur sculpteur du XVIIeme siècle. In *French Bronze Sculpture: Materials and Techniques 16th-18th Century*; Archetype: Paris, France, 2014; pp. 1–17.
27. Lombardi, G.; Vidale, M. From the shell to its content: The casting cores of the two bronze statues from Riace (Calabria, Italy). *J. Archaeol. Sci.* **1998**, *25*, 1055–1066. [CrossRef]
28. Lanterna, G. Multidisciplinary scientific analysis on restoration of a Renaissance masterpiece: Verrocchio's "L'Incredulita di san tommaso'', outdoor bronze group of Orsammichele Church in Florence. A case history. *Termochemica Acta* **1995**, *269*, 729–742. [CrossRef]
29. Pouyet, E.; Ganio, M.; Motlani, A.; Saboo, A.; Casadio, F.; Walton, M. Casting Light on 20th-Century Parisian Artistic Bronze: Insights from Compositional Studies of Sculptures Using Hand-Held X-ray Fluorescence Spectroscopy. *Heritage* **2019**, *2*, 732–748. [CrossRef]
30. Cartechini, L.; Rinaldi, R.; Kockelmann, W.; Bonamore, S.; Manconi, D.; Borgia, I.; Rocchi, P.; Brunetti, B.; Sgamellotti, A. Non-destructive characterization of compositional and textural properties of Etruscan bronzes: A multi-method approach. *Appl. Phys. A-Mater. Sci. Process.* **2006**, *83*, 631–636. [CrossRef]
31. Ropret, P.; Kosec, T. Outdoor Bronze and Its Protection. *Raman Spectrosc. Archaeol. Art Hist.* **2019**, *2*, 196–212.
32. Picciochi, R.; Ramos, A.C.; Mendonça, M.H.; Fonseca, I.T.E. Influence of the environment on the atmospheric corrosion of bronze. *J. Appl. Electrochem.* **2004**, *34*, 989–995. [CrossRef]
33. Robbiola, L.; Blengino, J.M.; Fiaud, C. Morphology and mechanisms of formation of natural patinas on archaeological Cu-Sn alloys. *Corros. Sci.* **1998**, *40*, 2083–2111. [CrossRef]

34. Robbiola, L.; Portier, R. A global approach to the authentication of ancient bronzes based on the characterization of the alloy–patina–environment system. *J. Cult. Herit.* **2006**, *7*, 1–12. [CrossRef]

35. FitzGerald, K.P.; Nairn, J.; Skennerton, G.; Atrens, A. Atmospheric corrosion of cooper and the colour, structure and composition of natural patinas on copper. *Corros. Sci.* **2006**, *48*, 2480–2509. [CrossRef]

36. de Oliveira, F.J.R.; Lago, D.C.B.; Senna, L.F.; de Miranda, L.R.M.; d'Elia, E. Study of patina formation on bronze specimens. *Mater. Chem. Phys.* **2009**, *115*, 761–770. [CrossRef]

37. Chiavari, C.; Colledan, A.; Frignani, A.; Brunoro, G. Corrosion evaluation of traditional and new bronzes for artistic castings. *Mater. Chem. Phys.* **2006**, *95*, 252–259. [CrossRef]

38. Ingo, G.M.; de Caro, T.; Riccucci, C.; Khosroff, S. Uncommon corrosion phenomena of archaeological bronze alloys. *Appl. Phys. A Mater. Sci. Process.* **2006**, *83*, 581–588. [CrossRef]

39. Domenic-Carbo, A.; Domenic-Carbo, M.T.; Martinez-Lazaro, I. Electrochemical identification of corrosion products in archaeological artefacts. A case study. *Microchim. Acta* **2007**, *162*, 351–359. [CrossRef]

40. Chelaru, J.D.; Soporan, V.F.; Nemeş, O. Time analysis of King Matthias the I Sculptural Group. *Int. J. Conserv. Sci.* **2010**, *1*, 69–74.

41. Sabau, J.D.; Muresan, L.M.; Soporan, V.F.; Nemes, O.; Kolozsi, T. A Study on the Corrosion Resistance of Bronzes Covered with Artificial Patina. *Int. J. Conserv. Sci.* **2011**, *2*, 109–116.

42. Casaletto, M.P.; Ingo, G.M.; Albini, M.; Lapenna, A.; Pierige, I.; Riccucci, C.; Faraldi, F. An integrated analytical characterization of corrosion products on ornamental objects from the necropolis of Colle Badetta-Tortoreto (Teramo, Italy). *Appl. Phys. Amater. Sci. Process.* **2010**, *100*, 801–808. [CrossRef]

43. Mureşan, L.; Varvara, S.; Stupnišek-Lisac, E.; Otmačić, H.; Marušić, K.; Takenouti, H. Protection of bronze covered with patina by innoxiouus organic substances. *Electrochim. Acta* **2007**, *52*, 7770–7779. [CrossRef]

44. Vlasa, A.; Varvara, S.; Mureşan, L. Electrochemical investigation of the influence of two thiadiazole derivatives on the patina of an artchaeological bronze artefact using a carbon paste electrode. *Stud. Univ. Babeş-Bolyai* **2007**, *2*, 63–71.

45. Kipper, P. *Patina for Silicon Bronze*; Regal Printing: Hong Kong, 2003.

46. Souissi, N.; Bousselmi, L.; Khosrof, S.; Triki, E. Electrochemical behavior of an archaeological bronze alloy in various aqueous media: New method for understanding artifacts preservation. *Mater. Corrsion* **2003**, *54*, 318–325. [CrossRef]

47. Privitera, A.; Corbascio, A.; Calcani, G.; Della Ventura, G.; Ricci, M.A.; Sodo, A. Raman approach to the forensic study of bronze patinas *J. Archaeol. Sci. Rep.* **2021**, *39*, 103115. [CrossRef]

48. Satovic, D.; Martinez, S.; Bobrowski, A. Electrochemical identification of corrosion products on historical and archaeological bronzes using the voltammetry of micro-particles attached to a carbon paste electrode. *Talanta* **2010**, *81*, 1760–1765. [CrossRef] [PubMed]

49. Kosec, T.; Curkovic, H.O.; Legat, A. Investigation of the corrosion protection of chemically and electrochemically formed patinas on recent bronze. *Electrochim. Acta* **2010**, *56*, 722–731. [CrossRef]

50. Noli, F.; Misaelides, P.; Hatzidimitriou, A.; Pavlidou, E.; Kokkoris, M.M. Investigation of artificially produced and natural copper patina layers. *J. Mater. Chem.* **2003**, *13*, 114–120. [CrossRef]

51. Doménech-Carbó, A.; Ramírez-Barat, B.; Petiti, C.; Goidanich, S.; Doménech-Carbó, M.T.; Cano, E. Characterization of traditional artificial patinas on copper using the voltammetry of immobilized particles. *J. Electroanal. Chem.* **2020**, *877*, 114494. [CrossRef]

52. Sandu, I.; Mircea, O.; Sandu, I.G.; Vasilache, V.; Sandu, A.V. Liesegang Effect Typology on Ancient Bronzes Discovered in Romania. *Rev. Chim.* **2014**, *65*, 311–319.

53. Sandu, I.; Mircea, O.; Sandu, I.G.; Vasilache, V. The Liesegang Effect on Ancient Bronze Items Discovered in Romania. *Int. J. Conserv. Sci.* **2013**, *4*, 573–586.

54. Sandu, I.G.; Mircea, O.; Vasilache, V.; Sandu, I. Influence of archaeological environment factors in alteration processes of copper alloy artifacts. *Microsc. Res. Tech.* **2012**, *75*, 1646–1652. [CrossRef] [PubMed]

55. Sandu, I.G.; Stoleriu; Sandu, I.; Brebu, M.; Sandu, A.V. Authentication of ancient bronze coins by the study of the archaeological patina. I. Composition and structure. *Rev. Chim.* **2005**, *56*, 981–994.

56. Scott, D.A. *Copper and Bronze in Art: Corrosion, Colorants and Conservation*, 1st ed.; Paul Getty Conservation Institute: Los Angeles, CA, USA, 2002; pp. 139–141.

57. Hughes, R.; Rowes, M. *The Colouring, Bronzing and Patination of Metals, Crafts*, 2nd ed.; Thames and Hudson: London, UK, 1991.

58. Balta, I.Z.; Robbiola, L. Study of black patinas on copper and bronze obtained by using 19th century western traditional techniques of artificial patination. In Proceedings of the 8th International Conference on Non-destructive Investigations and Microanalysis for the Diagnostics and Conservation of the Cultural and Environmental Heritage, Lecce, Italy, 5–19 May 2005.

59. Noli, F.; Misaelides, P.; Pavlidou, E.; Kokkoris, M. Investigation of copper patinas using ion beam analysis and scanning electron microscopy. *J. Surf. Interface Anal.* **2005**, *37*, 288–293. [CrossRef]

60. Cicileo, G.P.; Crespo, M.A.; Rosales, B.M. Comparative study of patinas formed on statuary alloys by means of electrochemical and surface analysis techniques. *Corros. Sci.* **2004**, *46*, 929–953. [CrossRef]

61. Crippa, M.; Bongiorno, V.; Piccardo, P.; Carnasciali, M.M. A Characterisation Study on Modern Bronze Sculpture: The Artistic Patinas of Nado Canuti. *Stud. Conserv.* **2019**, *64*, 16–23. [CrossRef]

62. Kwon, H. Corrosion Behaviors of Artificial Chloride Patina for Studying Bronze Sculpture Corrosion in Marine Environments. *Coatings* **2023**, *13*, 1630. [CrossRef]

63. Gianni, L. Corrosion Behavior of Bronze Alloys Exposed to Urban and Marine Environment: An Innovative Approach to Corrosion Process Understanding and to Graphical Results Presentation. Ph.D. Thesis, University of Ghent, Ghent, Belgium, 2011; pp. 7–27.
64. Sabbe, P.J.; Dowsett, M.G.; De Keersmaecker, M.; Hand, M.; Thompson, P.; Adriaens, A. Synthesis and surface characterization of a patterned cuprite sample: Preparatory step in the evaluation scheme of an X-ray-excited optical microscopy system. *Appl. Surf. Sci.* **2015**, *332*, 657–664. [CrossRef]
65. Balta, I.Z.; Pederzoli, S.; Iacob, E.; Bersani, M. Dynamic secondary ion mass spectrometry and X-ray photoelectron spectroscopy on artistic bronze and copper artificial patinas. *Appl. Surf. Sci.* **2009**, *255*, 6378–6385. [CrossRef]
66. Municchia, A.C.; Bellatreccia, F.; D'Ercoli, G.; Mastro, S.L.; Reho, I.; Ricci, M.A.; Sodo, A. Characterisation of artificial patinas on bronze sculptures of the Carlo Bilotti Museum (Rome). *Appl. Phys. A* **2016**, *122*, 1021. [CrossRef]
67. Stranges, F.; La Russa, M.; Oliva, A.; Galli, G. Analysis of the Quintilii's Villa Bronzes by Spectroscopy Techniques. *J. Archaeol.* **2014**, *2014*, 312981. [CrossRef]
68. Wells, C. *Scanning Electron Microscopy*; McGraw-Hill: New York, NY, USA, 1974.
69. Kuo, J. *Electron Microscopy: Methods and Protocols*, 2nd ed.; Humana Press: New Jersey, NJ, USA, 2007.
70. Tanasa, P.O.; Sandu, I.; Vasilache, V.; Sandu, I.G.; Negru, I.C.; Sandu, A.V. Authentication of a Painting by Nicolae Grigorescu Using Modern Multi-Analytical Methods. *Appl. Sci.* **2020**, *10*, 3558. [CrossRef]
71. Sandu, I.; Tanasa, O.; Negru, I.C.; Lupascu, M.-M.; Vasilache, V.; Chirila, M. Authentication of a Painting by Rene Magritte. *Int. J. Conserv. Sci.* **2022**, *13*, 1445–1462.
72. Sandu, I.; Lupascu, E.; Sandu, I.C.A.; Ivashko, Y. Artefactometrical Assessment of Works of ArtbBy Summing the Impact Grids of Altmetric Quantification. *Egypt. J. Archaeol. Restor. Stud.* **2023**, *13*, 185–196. [CrossRef]